

## Joukowski Airfoils

One of the more important potential flow results obtained using conformal mapping are the solutions of the potential flows past a family of airfoil shapes known as Joukowski foils. Like some of the other solutions presented here, we begin with a known solution, namely the flow past a circular cylinder with circulation and use conformal mapping to transform the cylinder into an airfoil shape. Thus we begin with what we choose to term the  $z'' = x'' + iy''$  plane shown in Figure 1. This  $z''$  plane contains the potential flow of a uniform stream,  $U$ , in the  $x''$  direction past a cylinder of radius,  $R$ , and circulation,  $\Gamma$ . The solution to the flow in this plane is therefore known and consists of the superposition of the complex potentials due to the uniform stream ( $f(z'') = Uz''$ ), due to the doublet at the origin ( $f(z'') = UR^2/z''$ ) and that due to the circulation ( $f(z'') = -i(\Gamma/2\pi) \ln z''/R$ ). Hence the solution in this plane is

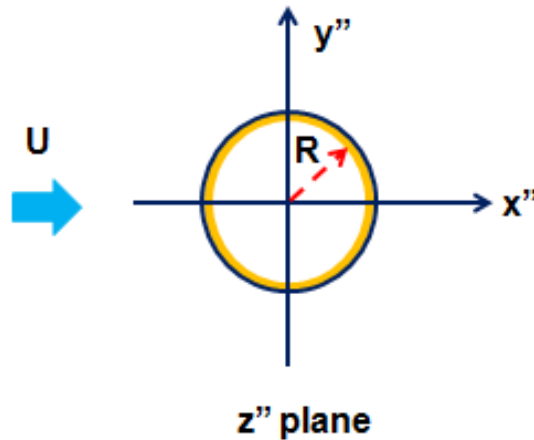


Figure 1: The  $z''$  plane: a cylinder in uniform stream.

$$f(z'') = Uz'' + \frac{UR^2}{z''} - i(\Gamma/2\pi) \ln z''/R \quad (\text{Bged1})$$

The second step in this four-step process is to add an angle of incidence,  $\alpha$ , by rotating the axes by that angle to achieve the geometry in the  $z' = x' + iy'$  plane shown in Figure 2. This transformation is achieved by the mapping

$$z' = z'' e^{i\alpha} \quad (\text{Bged2})$$

and it therefore follows that the flow in the  $z'$  plane is given by

$$f(z') = U \left\{ z' e^{-i\alpha} + \frac{R^2 e^{i\alpha}}{z'} \right\} - i \frac{\Gamma}{2\pi} \ln \left\{ \frac{z' e^{-i\alpha}}{R} \right\} \quad (\text{Bged3})$$

The third step introduces two crucial parameters that will determine the thickness and camber of the eventual airfoil even though it is not obvious at this point how this is achieved. Specifically we shift the center of the cylinder circle to a point in the second quadrant, namely the point  $a - Re^{-i\beta}$  where the significance of the parameters,  $a/R$  and  $\beta$  will not become clear until later. This displacement of the circle is achieved by the mapping  $z = z' + z_0$  which defines the  $z = x + iy$  plane where  $z_0 = a - Re^{-i\beta}$ . The  $z$

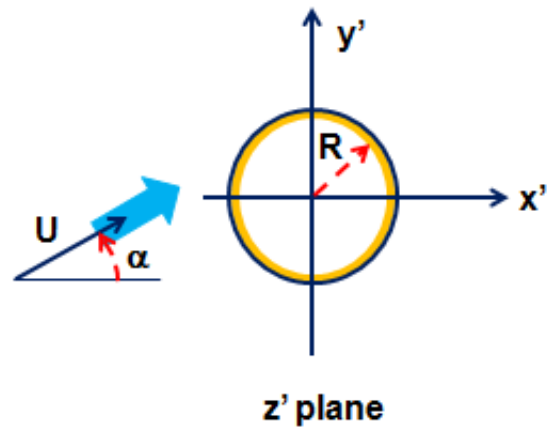


Figure 2: The  $z'$  plane with a rotation of  $\alpha$ .

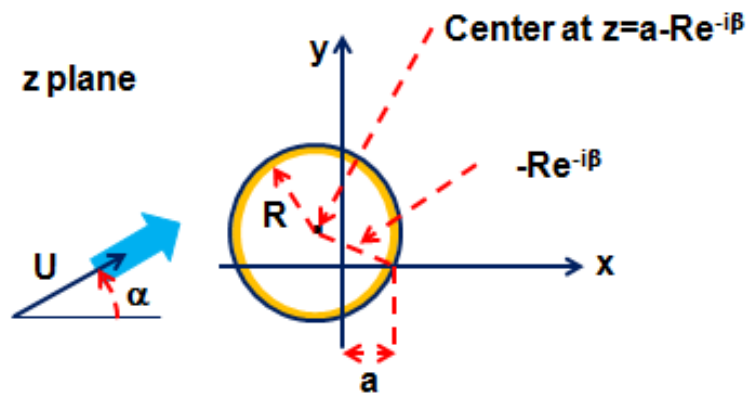


Figure 3: The  $z$  plane with a displacement of the cylinder.

plane is depicted in Figure 3 and it therefore follows that the flow in the  $z$  plane is given by

$$f(z) = Ue^{-i\alpha} \left\{ (z - z_0) + \frac{R^2 e^{2i\alpha}}{(z - z_0)} \right\} - i \frac{\Gamma}{2\pi} \ln \left\{ \frac{(z - z_0) e^{-i\alpha}}{R} \right\} \quad (\text{Bged4})$$

The fourth and final step is to apply the Joukowski mapping

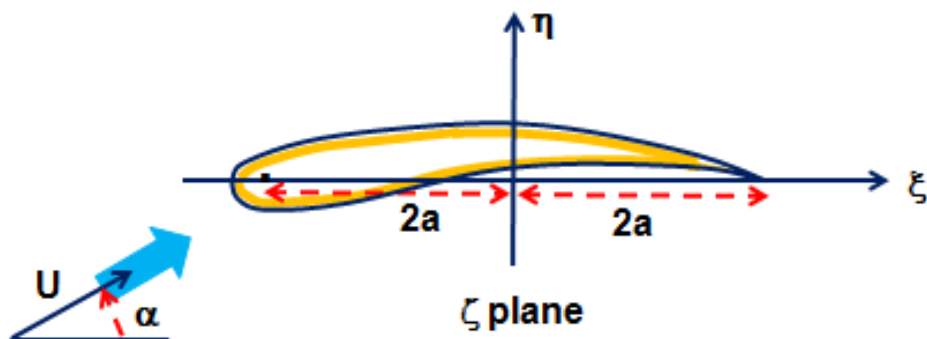


Figure 4: The  $\zeta$  plane of the Joukowski airfoil.

$$\frac{\zeta}{a} = \frac{z}{a} + \frac{a}{z} \quad (\text{Bged5})$$

which maps the circle in the  $z$  plane into the airfoil shape in the  $\zeta$  plane that is sketched in Figure 4.

Let us examine first the geometry of this Joukowski airfoil. First observe that the trailing edge of the foil is located at  $\zeta = 2a$  which corresponds to

$$z = a \quad , \quad z' = z - z_0 = Re^{-i\beta} \quad , \quad z'' = Re^{-i(\alpha+\beta)} \quad (\text{Bged6})$$

The surface of the “foil” in the  $z$  plane is a circle given parametrically by

$$\frac{z}{a} = 1 + \frac{R}{a} \{e^{i\theta} - e^{-i\beta}\} \quad (\text{Bged7})$$

for  $\theta = -\beta$  to  $\theta = 2\pi - \beta$ , those end points being the trailing edge. Therefore the profile of the Joukowski airfoil in the  $\zeta$  plane is given parametrically by

$$\frac{\zeta}{a} = 1 + \frac{R}{a} \{e^{i\theta} - e^{-i\beta}\} + \left[1 + \frac{R}{a} \{e^{i\theta} - e^{-i\beta}\}\right]^{-1} \quad (\text{Bged8})$$

for the same range of  $\theta$ . Clearly the two free parameters that determine the airfoil shape are  $R/a$  and  $\beta$ . It is readily shown that the parameter  $R/a$ , which must be greater than unity, determines the thickness of the foil. The thickness tends to zero as  $R/a$  is decreased towards unity. On the other hand the parameter  $\beta$  determines the camber (or baseline curvature) of the foil. Both of these parameter effects can be seen in the sample profiles presented in Figures 5 and 6. We should also note that all these Joukowski airfoils

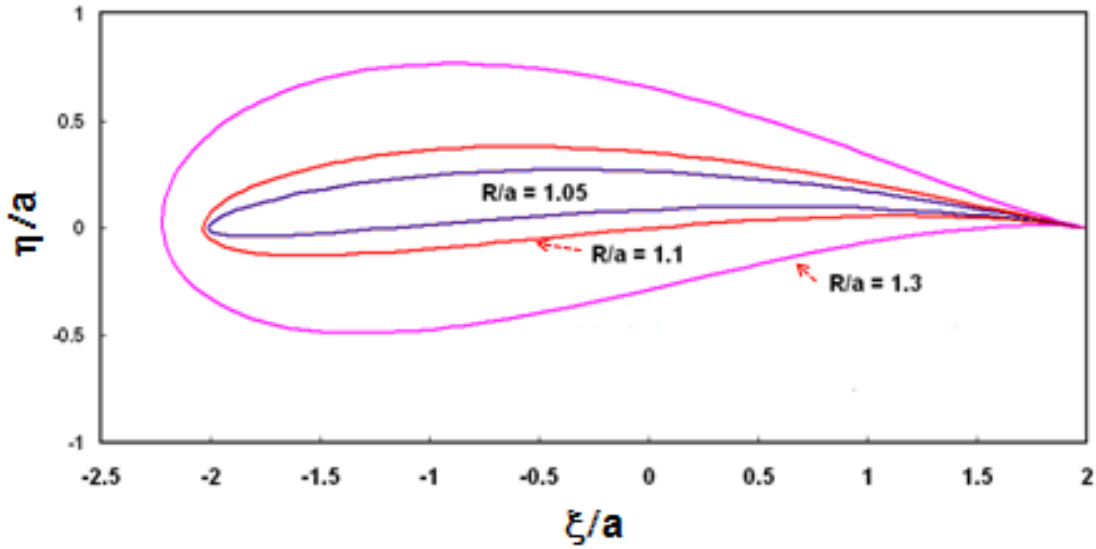


Figure 5: Joukowski airfoils for  $\beta = 5^\circ$  and  $\alpha = 5^\circ$ .

have profiles that have a cusp at the trailing edge. It can be shown that the tangent to the profile at this cusp makes an angle of  $2\beta$  to the  $\xi$  axis, a feature that is consistent with the fact that  $\beta$  determines the camber of the foil. One final aspect of the geometry needs to be noted. It can be shown from the profile given in equation (Bged8) (and is observed in Figures 5 and 6) that the leading edge is **not** located at  $\zeta = -2a$  but a short distance to the left of that point. The precise location and therefore the actual chord of the foil,  $c$ , must be determined numerically from the profile of equation (Bged8). Values of  $c/a$  for various  $R/a$  and several  $\beta$  are plotted in Figure 7. The distance from  $\zeta = -2a$  to the leading edge is

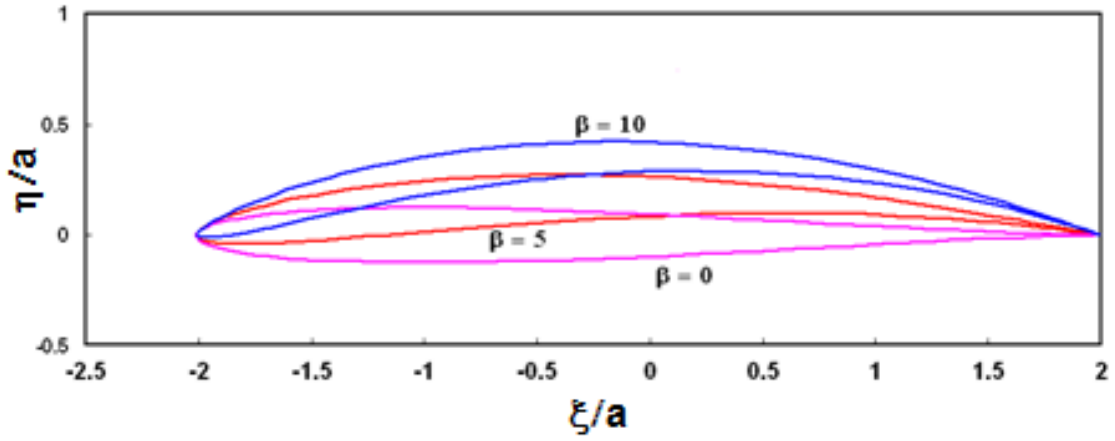


Figure 6: Joukowski airfoils for  $R/a = 1.05$  and  $\alpha = 5^\circ$ .

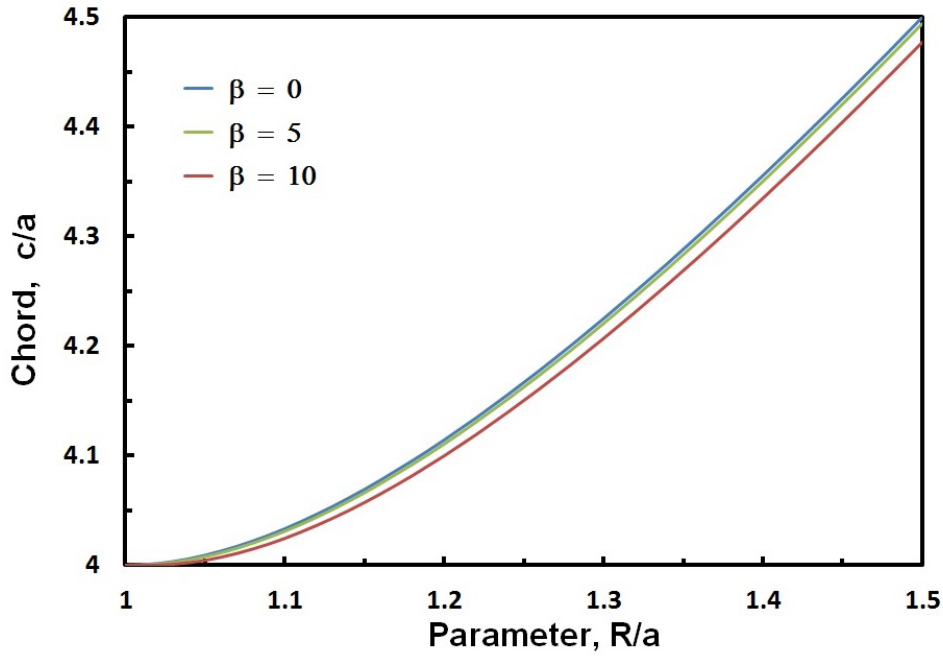


Figure 7: The values of  $c/a$  for various  $R/a$  and several  $\beta$ .

primarily a function of the foil thickness and therefore of the parameter  $R/a$  and  $c/a$  approaches the value of 4 as the thickness is reduced to zero ( $R/a \rightarrow 1$ ).

We also need to evaluate the velocity components on the surface of the foil, namely  $u_\xi$  and  $u_\eta$  which are given by

$$u_\xi - iu_\eta = \frac{df}{d\zeta} = \frac{df}{dz''} \frac{dz''}{dz'} \frac{dz'}{dz} \frac{dz}{d\zeta} \quad (\text{Bged9})$$

and evaluating each of these derivatives from the solution,  $f(z'')$ , and the mapping functions yields

$$u_\xi - iu_\eta = \left[ U \left\{ 1 - \frac{R^2}{z''^2} \right\} - \frac{i\Gamma}{2\pi z''} \right] e^{-i\alpha} \left\{ 1 - \frac{a^2}{z^2} \right\}^{-1} \quad (\text{Bged10})$$

Note first that, in general, the velocities approach infinity at the trailing edge  $z = a$ . This is because, in the general solution without further adjustment the flow negotiates the sharp trailing edge and we have

earlier seen, that a potential flow solution at a sharp projecting corner will have an infinite velocity at that point. This is an issue that we will address elsewhere in discussing viscous effects. For present purposes we will invoke the condition that in any real circumstance, the flow will not negotiate the trailing edge but will leave both surfaces of the foil smoothly, merging downstream. This special condition is called the *Kutta condition*; it is not inherent to potential flow but is invoked as a result of practical observation and supported by considerations of the viscous effects on the flow. If we apply the Kutta condition and require that the velocities be finite at the trailing edge then, according to equation (Bged10) this is only possible if

$$U \left\{ 1 - \frac{R^2}{z'^2} \right\} - \frac{i\Gamma}{2\pi z'} = 0 \quad \text{at } z = a, z' = Re^{-i(\alpha+\beta)} \quad (\text{Bged11})$$

or, if the circulation,  $\Gamma$ , is

$$\Gamma = -4\pi UR \sin(\alpha + \beta) \quad (\text{Bged12})$$

In other words there is just one value of the circulation for which the Kutta condition is satisfied and the flow leaves the trailing edge smoothly. Indeed, when we examine the potential flow solutions with circulations different from that of equation (Bged12) we find that those flows negotiate the trailing edge and have infinite velocities at that point.

Moreover, since the circulation determines the lift produced by the foil it follows that the Kutta condition is central to the process of producing lift. Indeed, the lift force,  $L$ , experienced by the foil per unit dimension normal to the plane of the flow is simply given by

$$L = -\rho\Gamma U = 4\pi\rho U^2 R \sin(\alpha + \beta) \quad (\text{Bged13})$$

in the direction perpendicular to the oncoming stream and upwards in Figure 4. [We should note here that this text has consistently used the sign convention that the circulation is positive in the anticlockwise direction. However, in many texts the opposite convention is used when discussing airfoil performance.] This lift,  $L$ , implies a lift coefficient,  $C_L$ , based on the airfoil chord length,  $c$ , of

$$C_L = \frac{L}{\frac{1}{2}\rho c U^2} = 8\pi\rho U^2 \frac{R}{c} \sin(\alpha + \beta) \quad (\text{Bged14})$$

where, as previously described, the chord,  $c$ , needs to be evaluated from the foil profile ( $c/a$  is a little greater than 4). Typical values of the lift coefficient are plotted in Figure 8.

There are several important features of the above result for the lift that deserve to be emphasized. Note first that the parameter,  $\beta$ , in other words the camber or foil curvature, does not effect the magnitude of  $L$  but merely shifts the effective value of the angle of attack,  $\alpha$ . Moreover, the parameter  $R/a$ , in other words the thickness of the foil, does not appear to have any effect on  $L$ . In fact, the thickness or  $R/a$  does have an effects on the coefficient,  $C_L$ , since increasing the thickness increases the value of the chord length,  $c$ .

Note also that the rudimentary case of the potential flow around an infinitely thin flat plate at an angle of attack is generated in the limit  $R/a \rightarrow 1$ ,  $\beta = 0$  for which it is readily seen that  $c = 4R$  and  $C_L = 2\pi \sin\alpha$ . This solution will be further addressed in section (Dcd).

It is also useful to give a few examples of the pressure distributions around the foils for several angles of incidence and several profile shapes. From the expressions for the velocities in equation (Bged10) with the value of  $\Gamma$  substituted from equation (Bged12) it follows that the magnitude of the velocity on the surface of the foil is

$$[u_\xi^2 + u_\eta^2]^{\frac{1}{2}} = 2U \{ \sin\theta - \alpha + \sin\alpha + \beta \} |z| \{ |z - a^2/z| \}^{-1} \quad (\text{Bged15})$$

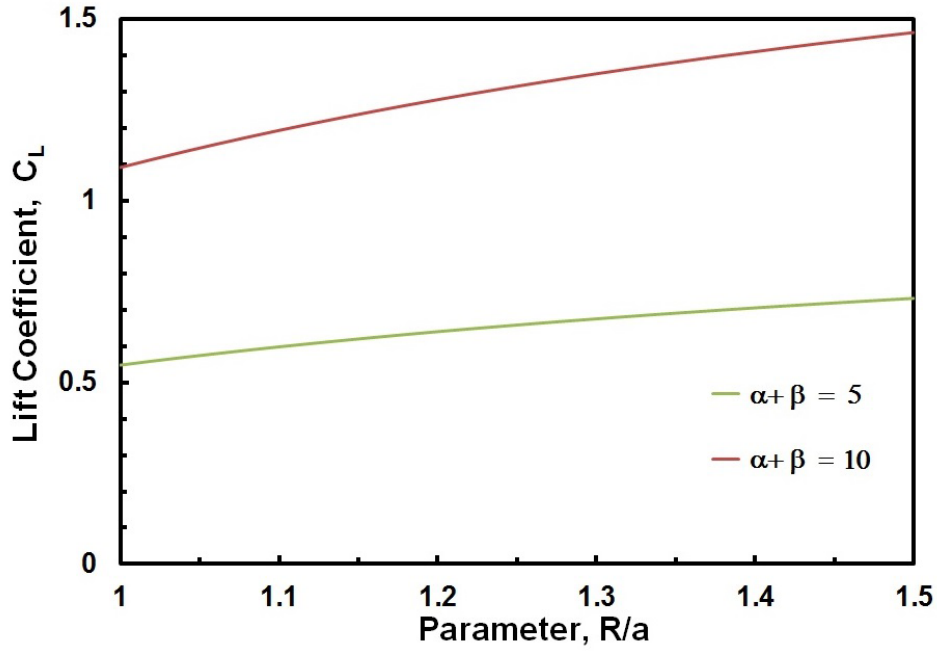


Figure 8: The lift coefficient,  $C_L$ , for various values of  $R/a$  and for two  $\alpha + \beta$ .

where, as previously discussed

$$\frac{z}{a} = 1 + \frac{R}{a} \{e^{i\theta} - e^{-i\beta}\} \quad (\text{Bged16})$$

for  $\theta = -\beta$  to  $\theta = 2\pi - \beta$ . Therefore the coefficient of pressure on the surface is given as

$$C_P = 1 - \frac{(u_\xi^2 + u_\eta^2)}{U^2} \quad (\text{Bged17})$$

Some typical pressure distributions on the surface of Joukowski airfoils (those shown in Figures 5 and 6) at an angle of attack of  $5^\circ$  are presented in Figures 9 and 10. The upper branch of the curves in these figures represent the pressure distribution on the pressure (or lower surface) of the foil while the lower branch is the distribution on the upper or suction surface of the foil. Note the location of the stagnation points on the pressure surface where  $C_P \rightarrow 1$ . Also note the minimum pressure points near the leading edge on the suction surface. That low pressure region is critical to the performance of actual airfoils because the details of the pressure distribution in that region can cause viscous boundary layer separation and/or transition to turbulence which, in turn, can lead to massive departures from the potential flow pressure distribution and airfoil performance. Airfoils must have rounded leading edges in order to minimize the effects of flow separation and the effect of thickness in reducing the depth of the pressure minimum is readily seen in Figures 9 and 10.

For later purposes in evaluating the added mass of Joukowski airfoils in section (Bmbe), we document several features of the above solution for potential flow about a Joukowski airfoil. When the value for the lift,  $\Gamma$ , from equation (Bged12) is substituted into the expression (Bged4) for the complex potential, the real part of that quantity, the velocity potential,  $\phi^*$  (the \* distinguishes this velocity potential from others developed later), becomes

$$\frac{\phi^*}{U} = \text{Re} \left\{ e^{-i\alpha} \left[ (z - z_0) + \frac{R^2 e^{2i\alpha}}{(z - z_0)} \right] + 2iR \sin(\alpha + \beta) \ln \left[ \frac{(z - z_0) e^{-i\alpha}}{R} \right] \right\} \quad (\text{Bged18})$$

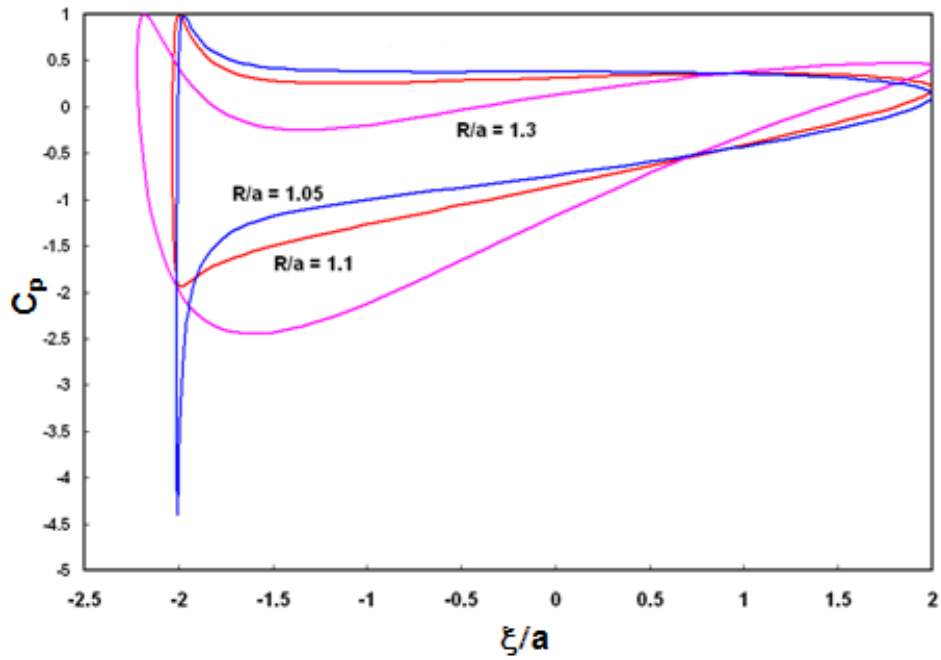


Figure 9: Surface coefficients of pressure for Joukowski airfoils with  $\beta = 5^\circ$  and  $\alpha = 5^\circ$ .

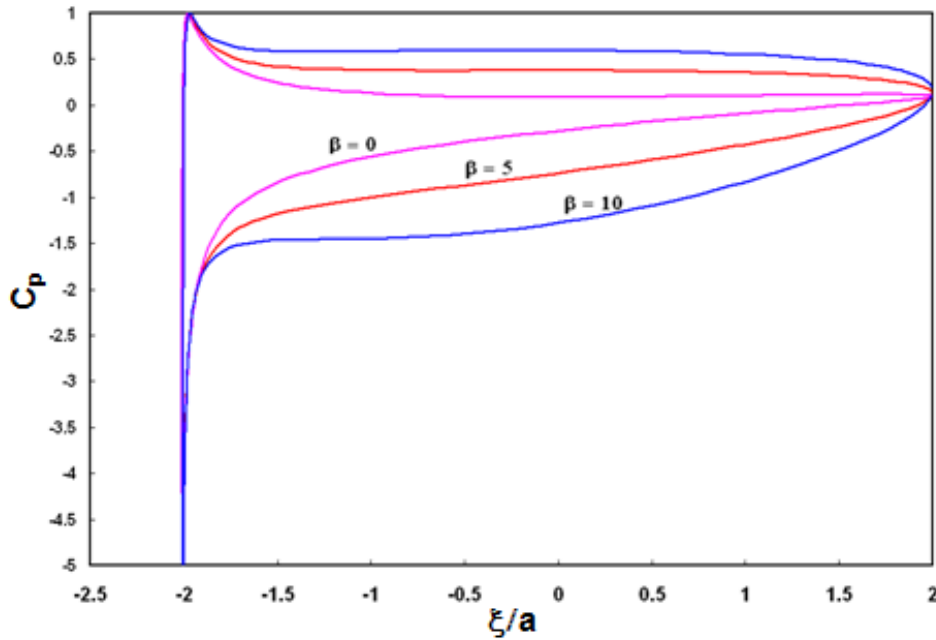


Figure 10: Surface coefficients of pressure for Joukowski airfoils with  $R/a = 1.05$  and  $\alpha = 5^\circ$ .

On the surface of the foil where  $z$  is given by equation (Bged7), it follows that the velocity potential,  $\phi^{**}$ , is

$$\frac{\phi^{**}}{Ua} = \frac{2R}{a} [\cos(\theta - \alpha) - (\theta - \alpha) \sin(\alpha + \beta)] \quad (\text{Bged19})$$

where the surface begins at the trailing edge at  $\theta = -\beta$  and ends at the trailing edge at  $\theta = 2\pi - \beta$ .